CANCER GENOMICS & PROTEOMICS 7: 337-346 (2010)

Effects of Artesunate on Cytokinesis and G_2/M Cell Cycle Progression of Tumour Cells and Budding Yeast

LISA STEINBRÜCK[1], GISLENE PEREIRA[2] and THOMAS EFFERTH[1,3]

[1]*Pharmaceutical Biology (C015) and* [2]*Molecular Biology of Centrosomes and Cilia (A180), German Cancer Research Center, Heidelberg, Germany;*
[3]*Department of Pharmaceutical Biology, Institute of Pharmacy and Biochemistry, University of Mainz, 55128 Mainz, Germany*

Abstract. *Artesunate, a semi-synthetic derivative of artemisinin, is an effective and safe anti-malaria drug, which also exhibits activity towards cancer cells. The present investigation studied the effect of artesunate on the mitosis of cancer and yeast cells by fluorescence microscopy and mRNA microarrays with a focus on the mitotic spindle checkpoint. The cytotoxicity of artesunate towards seven cell lines from six different cancer types was determined using the XTT assay. Furthermore, the cell cycle distribution of artesunate-treated cells was investigated by flow cytometry and immunofluorescence. To elucidate the genes mediating the effect of artesunate in the mitotic spindle checkpoint, knockout mutants of Saccharomyces cerevisiae were generated, since yeast knockouts are easier to generate than knockout strains of mammalian cells. Four out of the seven tested cell lines showed a G_2/M arrest upon artesunate exposure. Cells residing in the G_2/M arrest revealed multiple centrosomes, small multiple spindles and multi-nucleated cells, suggesting a defect in cytokinesis. The mitotic spindle checkpoint genes bub1, bub2, bub3, mad1, mad2 and mad3 were individually deleted and the sensitivity of these mutants towards artesunate was determined by monitoring the cell growth. The Δbub3 and Δmad3 mutants showed an increased sensitivity and the Δmad2 mutant a slightly decreased sensitivity to artesunate in comparison to the respective wild type. Bub3, Mad3 and Mad2 are the main regulators of the mitotic spindle checkpoint, suggesting that artesunate may interfere with this control mechanism.*

Correspondence to: Thomas Efferth, Department of Pharmaceutical Biology, Institute of Pharmacy and Biochemistry, University of Mainz, Staudinger Weg 5, 55128 Mainz, Germany. Tel: +49 61313925751, Fax: +49 61313923752, e-mail: efferth@uni-mainz.de/ Dr. Gislene Pereira, German Cancer Researh Center, Helmholtz Junior Research Group Molecular Biology of Centrosomes and Cilia, Im Neuenheimer Feld 581, 69120 Heidelberg, Germany. Tel: +49 6221423447, e-mail: g.pereira@dkfz-heidelberg.de

Key Words: Anticancer activity, artemisinin, cell cycle arrest, cytokinesis, mitotic checkpoint genes.

Cancer chemotherapy is often limited by severe side-effects and drug resistance. In an effort to overcome these limitations, there has been growing interest in the use of natural products derived from marine and terrestrial plants (1). Prominent examples of secondary plant metabolites used as anticancer agents are the *Vinca* alkaloids derived from *Catharanthus roseus,* the DNA topoisomerase I inhibitor camptothecin, derived from *Camptotheca acuminata,* the terpene paclitaxel, derived from *Taxus baccata,* and the lignan podophyllotoxin, isolated from *Podophyllum peltatum* (2).

Artemisinin is a sesquiterpene lactone that is widely used to treat drug-resistant malaria (3). To improve artemisinin's pharmacological properties, semi-synthetic derivatives have been developed, namely artemether, arteether and artesunate (4). Besides the activity against the malaria agents *Plasmodium falciparum* and *Plasmodium vivax*, artemisinin-type drugs are also active towards infections caused by *Schistosoma* (blood-flukes), *Pneumocystis carinii* (yeast-like fungal) (5), *Taxoplasma gondii* (parasitic protozoa) (6), hepatitis B virus (7) and human cytomegalovirus, as well as *Herpes* simplex virus (8). One major advantage of artemisinins is their lack of severe side-effects (9, 10).

In the 1990s, several groups reported the cytotoxic activity of artemisinin and its derivatives towards cancer (11-14). Among 55 tested tumour cell lines, leukaemia and colon cancer cells showed the highest sensitivity and non-small cell lung cancer the lowest sensitivity (15). Furthermore, two patients suffering from uveal melanoma were treated with artesunate in combination with standard chemotherapy and showed promising results (16). Although progress has been made in understanding the anti-malarial mechanism of artesunate (17), the underlying mechanisms in cancer cytotoxicity seem to be multifactorial and are still incompletely understood (18).

Artesunate's action in *Plasmodium* relies at least in part on the induction of reactive oxygen species (ROS) (19). ROS are created by free iron (II), found in the food vacuole of the parasite, reacting with the endoperoxide bridge of artesunate.

In *Plasmodium*, ROS damage of membranes leads to auto-digestion. Similar results were obtained for cancer cells. Artesunate-induced ROS also cause apoptosis in leukaemia T-cells by inducing the mitochondrial pathway (20). Interestingly, tumour cells contain more iron than normal cells (21) and their expression of CD71 transferrin receptor, which induces cellular uptake of the iron-transferrin complex, is also increased (22). These observations suggest that induction of ROS in tumour cells can be targeted selectively by combination of artesunate and transferrin or iron(II) glycine sulfate (Ferrosanol®) (4, 23). Apoptosis was also induced by artesunate *via* p53-dependent and -independent pathways (22, 24). Besides its apoptotic activities, artesunate also induces DNA double-strand breaks (25) and inhibits the Wnt/β-catenin pathway (26, 27). Furthermore, artesunate inhibits angiogenesis mainly by down-regulation of the vascular endothelial growth factor (VEGF) (28, 29).

Recent studies also revealed an effect of artesunate on the cell cycle. Cells overexpressing the cell division cycle 25A gene (*cdc25a*) showed increased artesunate sensitivity. CDC25A regulates the cell cycle progression from the G_1 to the S phase and was expressed less upon artesunate treatment (24). Furthermore, cells expressing high levels of the translationally controlled tumour protein (TCTP) were more sensitive to artesunate, while a low TCTP level was related to resistance (4). TCTP probably plays a role in cell cycle progression and regulation. During interphase and metaphase, TCTP binds to tubulin, whereas TCTP detaches from tubulin during the meta- to anaphase transition (30, 31). Overexpression of TCTP was related to microtubule stabilisation and a reduced growth rate *in vivo* (31). Additionally, TCTP is phoshorylated by the polo-like kinase 1 (Plk1), possibly making it a key target for regulation of anaphase progression (32). Recently, Jiao *et al.* (33) demonstrated that dihydroartemisinin, which is the active metabolite of artesunate, induces a dose-dependent cell cycle arrest in the G_2 phase. These findings possibly relate to the observation that a yeast strain lacking the mitotic spindle checkpoint gene *bub3* has increased sensitivity to artesunate (15). Bub3 is part of the mitotic spindle checkpoint controlling the progression from metaphase to anaphase (34). Thereby, Bub3, BubR1 (Mad3 in yeast) and Mad2 prevent binding of Cdc20 to the anaphase promoting complex (APC) until metaphase is completed. If the attachment of the microtubule spindle to the kinetochores of the chromosomes is performed correctly, Cdc20 is released and binds to the APC, inducing the cleavage of the sister chromatids. Thus, the mitotic spindle checkpoint is a key control mechanism of mitosis and a possible target of artesunate.

The present investigation focused on the effect of artesunate on mitosis, especially the mitotic spindle checkpoint. Seven cell lines from six different cancer types were analysed for their cytotoxicity, cell cycle arrest and apoptosis induction upon artesunate treatment. To elucidate the genes mediating artesunate's effect in the mitotic spindle checkpoint, knockout mutants of *Saccharomyces cerevisiae* were generated, since yeast knockouts are easier to generate than knockout strains of mammalian cells. It was found that the *bub3, mad3* and *mad2* genes are involved in artesunate's action. As a next step, *bub* and *mad* genes were investigated in human tumour cell lines. The microarray-based mRNA expressing human *mad2* gene correlated significantly with the response of the NCl cell line panel towards artesunate.

Materials and Methods

Human cancer cell culture. RPMI-1640 and DMEM were supplemented with 10% foetal bovine serum (FBS) and 1% of 10,000 U/ml Penicillin G- and 10 mg/ml streptomycin-containing solution. Leukaemia (J-Jhan and J16), small cell lung carcinoma (H69) and prostate carcinoma cells (DU145) were cultured in RPMI-1640-rich medium and colon carcinoma (HCT116), glioma (U251) and melanoma (SK-Mel-28) cells in DMEM-rich medium at 37˚C, 5% CO_2 and 95% relative humidity.

Cytotoxicity (XTT) assay. Artesunate was obtained from Saokim Ltd. (Hanoi, Vietnam). The XTT assay was performed as described previously (27). Briefly, the XTT assay is based on the metabolism of the yellow tetrazolium salt XTT (sodium 3'-[1-(phenylaminocarbonyl)-3,4-tetrazolium]-*bis*(4-methoxy-6-nitro) benzene sulfonic acid hydrate) to form the orange formazan dye accomplished by the mitochondrial dehydrogenases of viable cells. The amount of water-soluble formazan formed correlates directly to the number of living cells and was spectrophotometrically quantified with a microplate reader. The 50% inhibitory concentration values (IC_{50}) were determined from the logistic fit function using OriginPro7.5 software (OriginLab Corporation, Northampton, Massachusetts, USA).

Cell cycle analysis using propidium iodide (PI). A total of 1×10^5 adherent cells and 5×10^5 suspension cells were seeded in 12-well plates. Cells were treated with 0.26-260 μM artesunate for 6-96 h, untreated cells were used as positive control and DMSO served as vehicle control. Cells including the supernatant were harvested and fixed with 75% ice cold ethanol at –20˚C for at least 2 h. Cells were washed twice with 1 mM EDTA/PBS and the pellet was re-suspended in 100 μl PI staining solution (50 μg/ml PI, 0.1% w/v sodium citrate, 0.1% v/v Triton-X 100 and 1 mM EDTA in PBS). The cell cycle phase distribution was analysed by a FACS Calibur cytometer (Becton Dickinson, Heidelberg, Germany). Each experiment was performed at least in duplicate.

Immunofluorescence of human cancer cells. A total of 1×10^5 HCT116 and U251 cells were grown on glass coverslips. Cells were treated with 78 μM artesunate and incubated for 24 h or 48 h at 37˚C. Subsequently, the cells were fixed for 20 min with 4% PFA/PBS, permeabilised with 0.1% Triton X-100/PBS for 5 min at room temperature and quenched for 10 min using 0.12% glycine/PBS. After 15 min blocking with 3% BSA/PBS, cells were stained with primary antibodies containing rat-anti-α-tubulin (clone

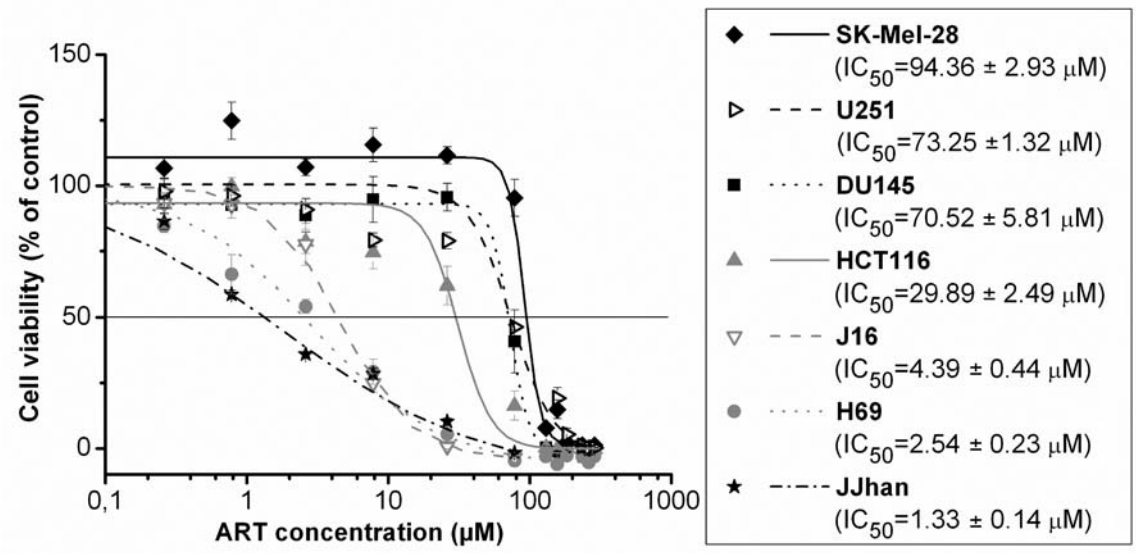

Figure 1. *Cytotoxicity of artesunate (ART) towards cancer cell lines. J16, J-Jhan, H69, DU145, SK-Mel-28, HCT116, and U251 cells were treated with artesunate (0-286 μM) for 72 h and subjected to the XTT-assay. Mean±SEM (standard error of the mean) of at least three independent experiments are shown. IC_{50} values were determined from the fitted-dose response curves. The leukaemia cell line J-Jhan was the most sensitive and the melanoma cell line SK-Mel-28 was the least sensitive towards artesunate.*

YL 1/2) and rabbit-anti-γ-tubulin (Sigma-Aldrich, Saint-Louis, MO, USA) and, subsequently, with secondary antibodies containing Alexa-594 goat-anti-rat and Alexa-488 goat-anti-rabbit (both obtained from Molecular Probes, Eugene, OR, USA). A total of 100-400 cells from each sample were analysed using a Zeiss Axiovert 200M (Carl Zeiss Europe, Jena, Germany) microscope (magnification ×63) and the MetaMorph Version 6.3 software (Molecular Devices, Inc., Sunnyvale, CA, USA). The experiments were performed in duplicate.

Yeast growth conditions, genetic manipulations and IC_{30} determination. Basic yeast methods were applied as described previously (35). Yeast strains were grown in yeast peptone dextrose medium with extra 0.1 mg/l adenine (YPAD). All yeast strains used were isogenic with S288C. PCR-based methods were used for gene deletions and epitope tagging (36). Chromosomal deletions were confirmed by colony PCR (36). *GFP-TUB1* strains were constructed using integration plasmids (37).

For IC_{30} determination, strains were grown in YPAD medium at 30˚C until a total of 1×10^7 cells/ml were achieved. Artesunate or DMSO were added and cultures were further incubated at 30˚C for 24 h. Cell growth was monitored by measuring the optical density (OD) at 600 nm (1 OD represents 2×10^7 cells/ml). Measurements were performed in triplicate from at least two independent experiments. The mean OD_{600} values and standard errors were calculated and normalised to control samples (DMSO treated). The mean values were plotted over the logarithmic artesunate concentration, and the data were fitted using the logistic function (Category Growth/Sigmoidal) of OriginPro 7.5 (OriginLab Corporation, Northampton/Massachusetts, USA). The IC_{30} values were calculated from the generated fit function (setting y=70). The IC_{30} errors were determined using the errors of the fit parameters and the Gaussian error calculus.

Microarray-based mRNA expression. The mRNA expression values for all human *bub* and *mad* genes of 55 cell lines were selected from the NCI database (http://dtp.nci.nih.gov). The mRNA expression was determined by microarray analysis (38). The IC_{50} values for artesunate of these 55 cell lines were previously reported (15). To show significant relationships between gene expression and artesunate response, the Fisher exact test was applied. This test was implemented into the WinSTAT Program (Kalmia, Cambridge, MA, USA).

Results

Cytotoxicity of different cell lines towards artesunate. In order to investigate the sensitivity of different human tumour cell lines towards artesunate, the IC_{50} values of seven cancer cell lines (J16, J-Jhan, H69, DU145, SK-Mel-28, HCT116, U251) originating from different organs were determined using the XTT assay. To this end, the cells were treated with increasing artesunate concentrations (ranging from 0-286 μM) and incubated for 72 h. All cell lines showed dose-dependent cytotoxicity (Figure 1). The human leukaemia cell lines J-Jhan and J16, as well as the small cell lung carcinoma cell line H69, were the most sensitive to artesunate (IC50 <5 μM), while the skin melanoma cell line SK-Mel-28 was the least responsive (IC_{50}=94 μM; Figure 1).

Effect of artesunate on cell cycle distribution. To determine whether artesunate has an effect on the cell cycle phase distribution, the seven cell lines were treated with 0.26-260 μM artesunate for 6-96 h at 37˚C and stained with propidium iodide. DMSO was tested as vehicle control. Figure 2

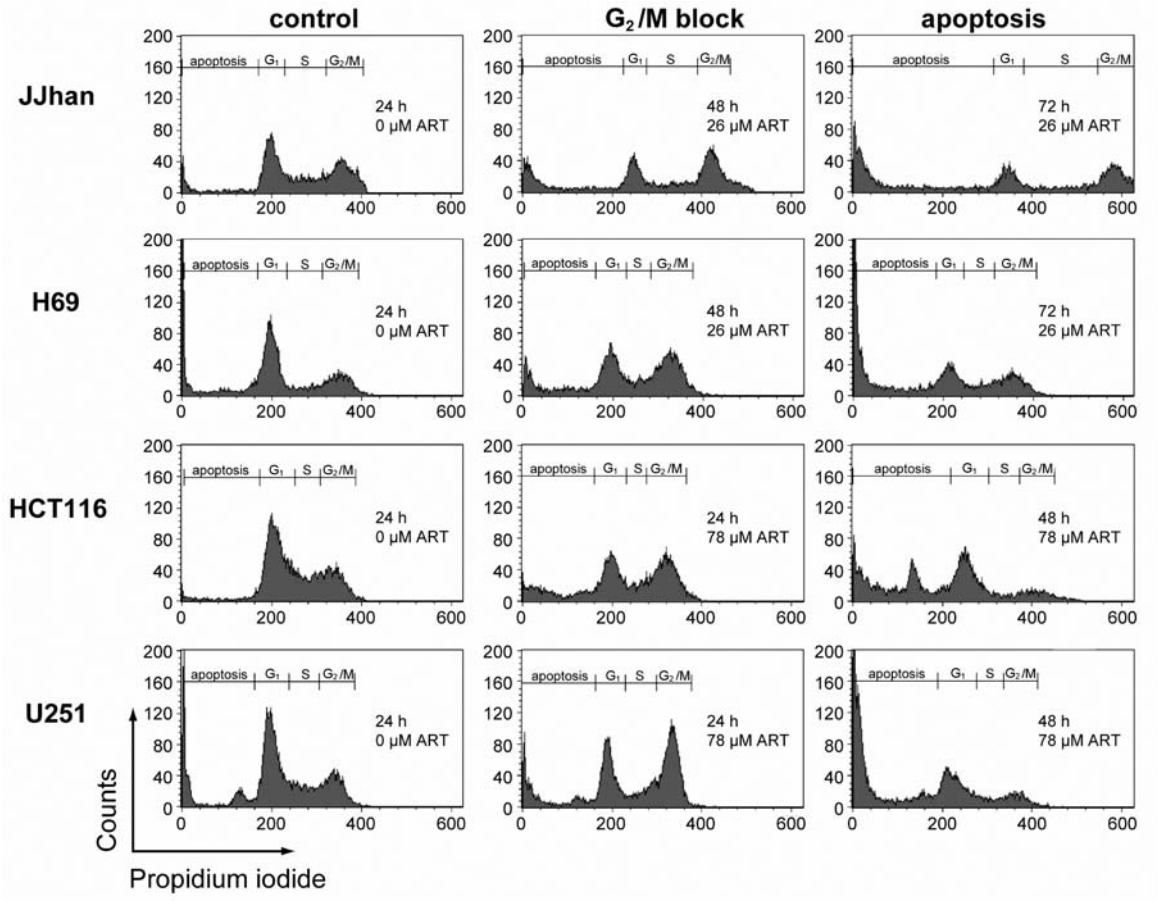

Figure 2. *Cell cycle distribution after artesunate (ART) treatment. J-Jhan, H69, HCT116, and U251 cells were treated with artesunate (0.26-260 μM), incubated at 37˚C for 6 h to 96 h, and stained with propidium iodide. The fluorescence intensity, representing the amount of cellular DNA, was measured by flow cytometry. Cell cycle distributions of untreated cells after 24 h were used as control. All depicted cell lines showed G_2/M arrest after incubation with 26 μM artesunate for 48 h (J-Jhan and H69) or with 78 μM artesunate for 24 h (HCT116 and U251). Further incubation led to increased apoptosis.*

displays results from two independent experiments. Artesunate induced a G_2/M arrest in four out of the seven cell lines, namely in J-Jhan, H69, HCT116 and U251 cells (Figure 2). This G_2/M block occurred for each cell line at certain treatment conditions and, thus, was highly dependent on the artesunate concentration and incubation time. Treatment for a prolonged incubation time or with higher artesunate concentrations, led to an increase of the apoptotic fraction in these cell lines. In contrast, J16, DU145 and SK-Mel-28 cells were not blocked in G_2/M and immediately underwent apoptosis (data not shown).

Ploidy of the used tumor cell lines. A common feature of cancer cell lines is their aneuploid genome. To determine whether the degrees of ploidy and artesunate sensitivities were correlated, normal peripheral blood mononuclear cells were used as a standard for diploid cells and the ploidy of the U251, DU145, SK-Mel-28 and HCT116 cell lines was evaluated by flow cytometry (Figure 3).

All cell lines tested were aneuploid having values of 4.4n (U251), 5.4n (HCT116), 7.1n (DU145) and 10.4n (SK-Mel-28). No correlation between the degree of ploidy and artesunate sensitivity or to the occurrence of G_2/M arrest was observed.

Phenotypes of artesunate-treated U251 and HCT116 cells. The artesunate-induced G_2/M arrest in U251 and HCT116 cells was analysed in more detail. Cells were seeded on cover-slips, treated with 78 μM artesunate and incubated for 24 h and 48 h at 37˚C. Microtubules and centrosomes were stained by immunofluorescence, DNA was counterstained with DAPI, and cells were analysed by fluorescence microscopy. To ensure that microscopically analysed cells represented cultures showing G2/M arrest, the cell cycle distribution was determined in parallel in the same samples (data not shown).

Eleven phenotypic categories were defined for U251 cells (Figure 4A and B). Besides the five typical mitotic phenotypes (interphase, prometaphase, metaphase, anaphase

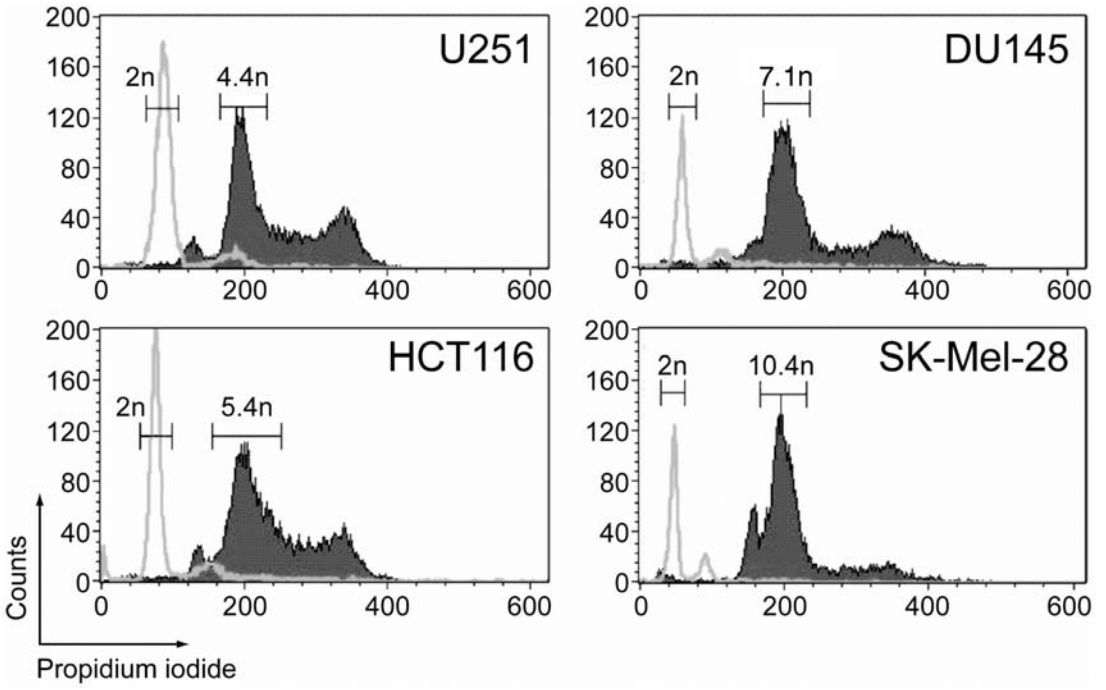

Figure 3. *Ploidy determination of cancer cells. The cell cycle phase distribution of untreated U251, HCT116, DU145 and SK-Mel-28 cells (dark) as well as healthy lymphocytes (light gray) was analysed by propidium iodide staining and flow cytometry in parallel. The ploidy of the lymphocytes in G_1 phase was set to 2n. The ploidy of the cancer cell lines was calculated from the G_1 marker means. All analysed cancer cell lines were aneuploid and possessed additional chromosomes.*

and telophase), six aberrant phenotypes appeared in U251 cells upon artesunate treatment (Figure 4B). The quantitative analysis is shown in Figure 4C. A minor phenotype of artesunate-treated cells was defined by very small and round cells possessing multiple spindles. This phenotype increased to 6% after 24 h and decreased to 1% after 48 h during further artesunate treatment. Untreated cells did not show this phenotype. 13% (24 h) and 29% (48 h) of artesunate-treated U251 cells revealed remote centrosomes in combination with large nuclei and missing spindle formation, which were not found in untreated cells. In addition, 16% (24 h) and 17% (48 h) of artesunate-treated cells exhibited two separated nuclei per cell while 6% (24 h) and 3% (48 h) of artesunate-treated cells exhibited two connected nuclei per cell. These phenotypes did not exceed 3% in untreated controls. Furthermore, artesunate-treated U251 cells were characterized by multiple centrosomes in combination with one or multiple nuclei. This phenotype reached 5% (24 h) and 18% (48 h) and was absent from untreated cells. All these phenotypes are characteristic for cytokinesis defects.

HCT116 cells were analysed in a similar manner to U251 cells. Not only did untreated HCT116 cells show the five normal mitosis phases, but they also showed cells which were linked by a thin cell connection (Figure 4D). Two additional aberrant phenotypes were observed (Figure 4E) with small round cells, collapsed microtubule cytoskeleton and one or multiple nuclei. 18% (24 h) and 50% (8 h) of artesunate-treated HCT116 cells showed one nucleus, whereas 49% (24h) and 20% (48 h) of artesunate-treated cells possessed multiple nuclei (Figure 4F). Both phenotypes were absent from untreated cells indicating that multi-nucleated HCT116 cells by artesunate treatment were caused by cytokinesis defects.

Effect of artesunate on budding yeast. Saccharomyces cerevisiae was used to determine whether the mitotic spindle checkpoint is a target for artesunate. To this end, yeast strains with knockouts in the mitotic checkpoint genes *bub1, bub2*, *bub3, mad1, mad2*, or *mad3* were prepared. A dose–response curve was determined by treating the different yeast strains with 0-600 μM artesunate for 24 h and measuring the OD_{600} value. As shown in Figure 5, the OD_{600} values of artesunate treated cells were never less than 50% of untreated control cells. Thus, IC_{30} instead of IC_{50} values were determined. The IC_{30} value of wild-type cells was 54±8 μM. The most sensitive mutants were *Δbub3* and *Δmad3,* with IC_{30} values of 33±6 μM and 38±9 μM, respectively. In contrast, *Δmad2* was slightly more resistant than the wild-type, with an IC_{30} value of 62±9 μM.

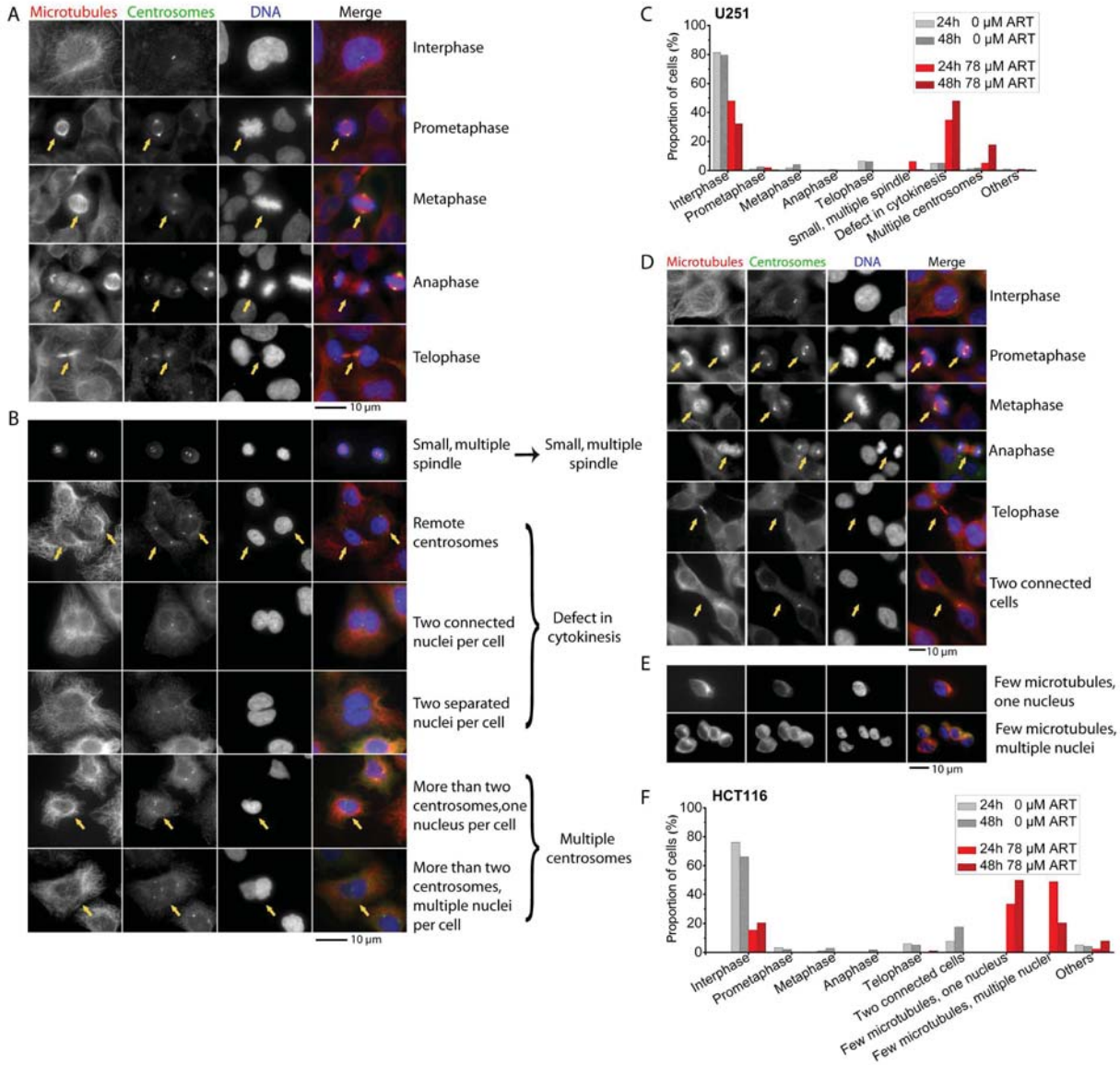

Figure 4. *Mitotic phenotypes of untreated and artesunate-treated U251 and HCT116 cells as assessed by confocal microscopy. Microtubules (red), centrosomes (green), and DNA (blue) were stained. A: Normal mitosis in untreated U251 cells. B: U251 cells showing abnormal cell phenotypes (predominantly observed in artesunate-treated cells). For quantitative analysis, the categories 'remote centrosomes', 'two connected nuclei per cell' and 'two separated nuclei per cell' were summarised as 'defect in cytokinesis'. Additionally, the categories 'more than two centrosomes, one nucleus per cell' and 'more than two centrosomes, multiple nuclei per cell' were grouped as 'multiple centrosomes'. C: Quantification of mitotic phenotypes shown in A and B. U251 cells were either untreated (gray) or treated with 78 µM artesunate (red) for 24 h (unshaded) or 48 h (shaded); 100-400 cells per sample were analysed by fluorescence microscopy. D: Normal mitosis in untreated HCT116 cells and an additional phenotype of two connected cells. E: HCT116 cells showing abnormal cell phenotypes (predominately observed in artesunate-treated cells) comprising few microtubules and one or multiple nuclei per cell. F: Quantification of mitotic phenotypes shown in D and E. HCT116 cells were either untreated (gray) or treated with 78 µM artesunate (red) for 24 h (unshaded) or 48 h (shaded); 100-400 cells per sample were analysed by fluorescence microscopy. The data represent the sum of two independent experiments.*

Association of mad2 expression and artesunate response in human cancer cell lines. To test whether these mitotic checkpoint genes may also be associated with the response of cancer cells towards artesunate, the microarray-based mRNA expression of all *bub* and *mad* genes in the human genome was correlated with the IC_{50} values for artesunate in 55 cell lines of different tumour types of the NCI drug screening panel. Only the *mad2*, human homologue: *madl1*, gene expression correlated significantly by means of the Fisher exact test with response to artesunate. For two *madl1* clones (GenBank

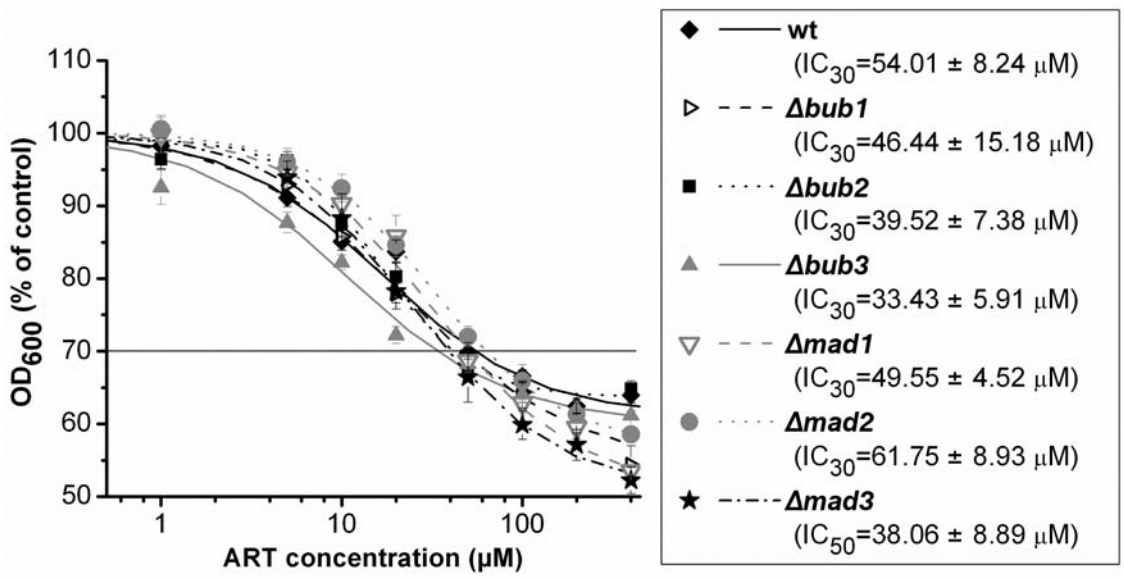

Figure 5. *Growth inhibition by artesunate in wild-type and knockout strains of S. cerevisiae. Wild-type, Δbub1, Δbub2, Δbub3, Δmad1, Δmad2, and Δmad3 yeast cells were treated with artesunate (0-600 μM) and incubated for 24 h. The OD_{600} was determined and normalised to 100% for untreated cells. The IC_{30} was calculated from the fitted dose-response curves. Mean±SEM (standard error of the mean) of at least two independent experiments are shown. The Δbub3 mutant was the most sensitive and the Δmad2 mutant was the least sensitive towards artesunate.*

Accession numbers U65410 and NM002358) significant inverse relationships were found (p=0.01 and p=0.03, respectively), indicating that high *madl1* expression is associated with sensitivity to artesunate (low IC_{30} values), and low expression is associated with resistance to artesunate (high IC_{30} values).

Discussion

Several studies have focused on the effects of artemisinin-like compounds on the cell cycle. The results are, however, not conclusive. While some authors have reported G_0/G_1 arrest upon artesunate treatment, others have found G_2/M block or no disturbance of the cell cycle at all (15, 24, 33, 39-41). Thus, the aim of this study was to investigate the effect of artesunate on the cell cycle of different cancer cell lines and on the mitotic spindle checkpoint in yeast. Seven cell lines from six different cancer types (leukaemia, small-cell lung cancer, glioma, melanoma, colon carcinoma and prostate carcinoma) were investigated. Intriguingly, only four out of the seven cell lines showed G_2/M arrest (J-Jhan, H69, HCT116, and U251). These cell lines may share still undefined genetic defects. J-Jhan, but not J16 showed G_2/M arrest, although both are sublines derived from the same parental Jurkat cell line. The artesunate-induced G_2/M arrest in U251 and HCT116 cells was analysed in more detail by confocal fluorescence microscopy. Aberrant phenotypes such as remote centrosomes, two connected nuclei per cell and two separated nuclei per cell, indicated that the cells duplicated DNA, as can be seen by a large nucleus or two nuclei per cell, but they are not able to divide physically. Therefore, these phenotypes were defined as cytokinesis defects.

Multiple centrosomes are common in cancer cells and lead to an assembly of multiple spindles (42). If the spindle possesses more than three poles due to the presence of multiple centrosomes, cytokinesis is impaired (43). In healthy cells, a cytokinesis failure activates *p53* leading to apoptosis (44). Since U251 cells (but not HCT116 cells) have a mutated *p53* gene, apoptosis cannot be activated directly, leading to either bi-nucleated or large mono-nucleated cells (43, 45). Both phenotypes were observed after artesunate treatment. HCT116 cells possibly bypassed apoptosis by a p53-independent pathway. Usually, in the G_1 phase each cell has one centrosome that is duplicated in the S phase, allowing the formation of a bipolar spindle. If a tumour cell is not physically divided during cytokinesis, it still contains at least two centrosomes in the following G_1 phase. However, if apoptosis is impaired and cell cycle progresses, the existing multiple centrosomes are duplicated, which in turn enhances the possibility of multiple spindles and thus a cytokinesis defect. Hence, it can be argued that excessive centrosomal amplification may induce cytokinesis defects or *vice versa* (43).

Further evidence that the growth inhibitory effect of artesunate may be correlated with a cell cycle defect arises from previously published data. Cells overexpressing the cell division cycle 25A gene (*cdc25a*) showed increased artesunate sensitivity. CDC25A regulates the cell cycle progression from G_1 to S phase and was less expressed upon artesunate treatment (24).

Furthermore, artesunate reduces the expression of *survivin* (26), which is part of the chromosomal passenger complex (CPC) also comprising the aurora B kinase, the inner centromere protein (INCENP) and borealin (46). CPC plays a key role in the regulation of mitosis, meiosis and cytokinesis (47). One function of survivin within CPC is targeting the complex to its different activity areas during cell division (48). As part of the mitotic spindle checkpoint, survivin and INCENP sense the tension between kinetochores and the spindle (49), thereby checking the correct spindle attachment. Furthermore, survivin regulates the Mad3 (BubR1) levels at kinetochores. Aurora B together with Bub1 maintain Mad3 (BubR1)-mediated inhibition of APC, which also belongs to the mitotic spindle checkpoint (46, 50-52). CPC interacts with the kinesin superfamily proteins (47) controlling cell division (53). Hence, it can be speculated that artesunate reduces survivin expression, which in turn impairs the correct cell cycle regulation, leading to defects in the mitotic spindle checkpoint and cytokinesis.

Besides CPC, Polo-like kinase 1 (Plk1) is also a key regulator of mitosis, meiosis and cytokinesis (54). *Plk1* knockout leads to mitotic G_2/M arrest, mono-polar spindles, and multi-nucleated cells (55). Furthermore, Plk1 phosphorylates TCTP, thereby regulating its localisation. TCTP plays a role in cell cycle progression and regulation (30). Cells highly expressing *tctp* are more sensitive to artesunate (4). Thus, artesunate may also affect cell cycle progression and cytokinesis *via* a connection to TCTP and Plk1.

Saccaromyces cerevisiae was applied to investigate the influence of artesunate on the mitotic spindle checkpoint. Yeast cells are widely used for cell cycle analysis, since they can be genetically manipulated easily in comparison to mammalian cells. Most importantly, the cell cycle machinery is conserved from yeast to humans (56, 57).

Six knockout yeast mutants of the mitotic spindle checkpoint genes, *bub1, bub2, bub3, mad1, mad2* or *mad3*, were generated by homologous recombination, and their sensitivity to artesunate was determined. All mutants except for *Δmad2* were more sensitive to artesunate than the wild-type. *Δbub3* showed the lowest IC_{30} value, consistent with published results (15). The IC_{30} values of *Δbub3, Δmad3* and *Δmad2* differed significantly from the respective wild-type values. Interestingly, these proteins are important regulators of the mitotic spindle checkpoint and prevent the binding of Cdc20 to anaphase-promoting complex (APC) until all kinetochores are correctly attached to the spindle. These results suggest that artesunate may interfere with the mitotic spindle checkpoint.

The sensitivity of the *Δbub3* mutant towards artesunate may be due to artesunate-induced reduced *survivin* expression (26) in analogy to human cancer cells. Survivin regulates BubR1 levels (the vertebrate homologue of Mad3) at the kinetochores. Therefore, it can be speculated that artesunate may influence BubR1 (Mad3) indirectly by down-regulating survivin expression. Bub3 binds to Mad3 in the active mitotic checkpoint. Mad3 may be able to maintain the mitotic spindle checkpoint in the absence of Bub3 without artesunate treatment. This is supported by the observation that the *Δbub3* mutant grew normally in the absence of artesunate. However, upon artesunate exposure of the *Δbub3* mutant, Mad3 levels may be reduced (due to diminished expression of survivin induced by artesunate) and the Bub3/Mad3 complex may no longer be present. As the Bub3/Mad3 complex is important for recognition of free kinetochores (58), the absence of the complex may disturb the mitotic checkpoint and lead to reduced growth or even apoptosis. This might explain the high sensitivity of the *Δbub3* mutant towards artesunate. Nevertheless, survivin-independent signalling pathways may also contribute to this effect.

In summary, this study showed that artesunate induces a G_2/M block in four out of the seven tested cell lines. The G_2/M block was dependent on artesunate concentration and incubation time. Furthermore, the phenotypes of cells residing in this block (multiple centrosomes, multiple spindle and multinucleated cells) suggested that artesunate causes a defect in cytokinesis. A deletion of the mitotic spindle checkpoint genes *bub3* and *mad3* in budding yeast led to an increased sensitivity towards artesunate, which also suggested that artesunate interferes with cell cycle progression.

Acknowledgements

This work of G.P. is funded by Helmholtz Association grant (HZ-NG-111) and Maria Curie Excellence Grant (MEXT-CT-2006-042544).

References

1 Cragg GM, Newman DJ and Yang SS: Natural product extracts of plant and marine origin having antileukemia potential. The NCI experience. J Nat Prod *69*: 488-498, 2006.

2 Boik J: Natural compounds in cancer therapy. Oregon Medical Press, 2001.

3 Yeung S, Pongtavornpinyo W, Hastings IM, Mills AJ and White NJ: Antimalarial drug resistance, artemisinin-based combination therapy, and the contribution of modeling to elucidating policy choices. Am J Trop Med Hyg *71*: 179-186, 2004.

4 Efferth T: Mechanistic perspectives for 1,2,4-trioxanes in anti-cancer therapy. Drug Resist Updat *8*: 85-97, 2005.

5 Merali S and Meshnick SR: Susceptibility of *Pneumocystis carinii* to artemisinin *in vitro*. Antimicrob Agents Chemother *35*: 1225-1227, 1991.

6 Ke OY, Krug EC, Marr JJ and Berens RL: Inhibition of growth of *Toxoplasma gondii* by qinghaosu and derivatives. Antimicrob Agents Chemother *34*: 1961-1965, 1990.

7 Romero MR, Efferth T, Serrano MA, Castano B, Macias RI, Briz O and Marin JJ: Effect of artemisinin/artesunate as inhibitors of hepatitis B virus production in an '*in vitro*' replicative system. Antiviral Res *68*: 75-83, 2005.

8 Efferth T, Marschall M, Wang X, Huong SM, Hauber I, Olbrich A, Kronschnabl M, Stamminger T and Huang ES: Antiviral activity of artesunate towards wild-type, recombinant, and ganciclovir-resistant human cytomegaloviruses. J Mol Med *80*: 233-242, 2002.
9 Ribeiro IR and Olliaro P: Safety of artemisinin and its derivatives. A review of published and unpublished clinical trials. Med Trop (Mars) *58*: 50-53, 1998.
10 Efferth T and Kaina B: Toxicity of the antimalarial artemisinin and its derivatives. Crit Rev Toxicol *40*: 405-421, 2010.
11 Woerdenbag HJ, Moskal TA, Pras N, Malingre TM, el-Feraly FS, Kampinga HH and Konings AW: Cytotoxicity of artemisinin-related endoperoxides to Ehrlich ascites tumor cells. J Nat Prod *56*: 849-856, 1993.
12 Zheng GQ: Cytotoxic terpenoids and flavonoids from *Artemisia annua*. Planta Med *60*: 54-57, 1994.
13 Lai H and Singh NP: Selective cancer cell cytotoxicity from exposure to dihydroartemisinin and holotransferrin. Cancer Lett *91*: 41-46, 1995.
14 Efferth T, Rücker G, Falkenberg M, Manns D, Olbrich A, Fabry U and Osieka R: Detection of apoptosis in KG-1a leukemic cells treated with investigational drugs. Arzneimittelforschung *46*: 196-200, 1996.
15 Efferth T, Dunstan H, Sauerbrey A, Miyachi H and Chitambar CR: The anti-malarial artesunate is also active against cancer. Int J Oncol *18*: 767-773, 2001.
16 Berger TG, Dieckmann D, Efferth T, Schultz ES, Funk JO, Baur A and Schuler G: Artesunate in the treatment of metastatic uveal melanoma first experiences. Oncol Rep *14*: 1599-1603, 2005.
17 Golenser J, Waknine JH, Krugliak M, Hunt NH and Grau GE: Current perspectives on the mechanism of action of artemisinins. Int J Parasitol *36*: 1427-1441, 2006.
18 Efferth T: Molecular pharmacology and pharmacogenomics of artemisinin and its derivatives in cancer cells. Curr Drug Targets *7*: 407-421, 2006.
19 Meshnick SR: The mode of action of antimalarial endoperoxides. Trans R Soc Trop Med Hyg *88(Suppl 1)*: S31-S32, 1994.
20 Efferth T, Giaisi M, Merling A, Krammer PH and Li-Weber M: Artesunate induces ROS-mediated apoptosis in doxorubicin-resistant T leukemia cells. PLoS ONE *2*: e693, 2007.
21 Shterman N, Kupfer B and Moroz C: Comparison of transferrin receptors, iron content and isoferritin profile in normal and malignant human breast cell lines. Pathobiology *59*: 19-25, 1991.
22 Efferth T, Benakis A, Romero MR, Tomicic M, Rauh R, Steinbach D, Hafer R, Stamminger T, Oesch F, Kaina B and Marschall M: Enhancement of cytotoxicity of artemisinins toward cancer cells by ferrous iron. Free Radic Biol Med *37*: 998-1009, 2004.
23 Kelter G, Steinbach D, Konkimalla VB, Tahara T, Taketani S, Fiebig HH and Efferth T: Role of transferrin receptor and the ABC transporters ABCB6 and ABCB7 for resistance and differentiation of tumor cells towards artesunate. PLoS ONE *2*: e798, 2007.
24 Efferth T, Sauerbrey A, Olbrich A, Gebhart E, Rauch P, Weber HO, Hengstler JG, Halatsch ME, Volm M, Tew KD, Ross DD and Funk JO: Molecular modes of action of artesunate in tumor cell lines. Mol Pharmacol *64*: 382-294, 2003.
25 Li PC, Lam E, Roos WP, Zdzienicka MZ, Kaina B and Efferth T: Artesunate derived from traditional Chinese medicine induces DNA damage and repair. Cancer Res *68*: 4347-4351, 2008.
26 Li LN, Zhang HD, Yuan SJ, Tian ZY, Wang L and Sun ZX: Artesunate attenuates the growth of human colorectal carcinoma and inhibits hyperactive Wnt/beta-catenin pathway. Int J Cancer *121*: 1360-1365, 2007.
27 Konkimalla VB, Blunder M, Korn B, Soomro SA, Jansen H, Chang W, Posner GH, Bauer R and Efferth T: Effect of artemisinins and other endoperoxides on nitric oxide-related signaling pathway in RAW 264.7 mouse macrophage cells. Nitric Oxide *19*: 184-191, 2008.
28 Dell'Eva R, Pfeffer U, Vene R, Anfosso L, Forlani A, Albini A and Efferth T: Inhibition of angiogenesis *in vivo* and growth of Kaposi's sarcoma xenograft tumors by the anti-malarial artesunate. Biochem Pharmacol *68*: 2359-2366, 2004.
29 Zhou HJ, Wang WQ, Wu GD, Lee J and Li A: Artesunate inhibits angiogenesis and down-regulates vascular endothelial growth factor expression in chronic myeloid leukemia K562 cells. Vascul Pharmacol *47*: 131-138, 2007.
30 Bommer UA and Thiele BJ: The translationally controlled tumour protein (TCTP). Int J Biochem Cell Biol *36*: 379-385, 2004.
31 Gachet Y, Reyes C, Goldstone S and Tournier S: The fission yeast spindle orientation checkpoint: a model that generates tension? Yeast *23*: 1015-1029, 2006.
32 Yarm FR: Plk phosphorylation regulates the microtubule-stabilizing protein TCTP. Mol Cell Biol *22*: 6209-6221, 2002.
33 Jiao Y, Ge CM, Meng QH, Cao JP, Tong J and Fan SJ: Dihydroartemisinin is an inhibitor of ovarian cancer cell growth. Acta Pharmacol Sin *28*: 1045-1056, 2007.
34 Diaz-Martinez LA and Yu H: Running on a treadmill: dynamic inhibition of APC/C by spindle checkpoint. Cell Div *2*: 23, 2007.
35 Stryer L, Berg JM, Tymoczko JL and Clarke NG: Biochemistry. W.H. Freeman and Co, 2002.
36 Janke C, Magiera MM, Rathfelder N, Taxis C, Reber S, Maekawa H, Moreno-Borchart A, Doenges G, Schwob E, Schiebel E and Knop M: A versatile toolbox for PCR-based tagging of yeast genes: new fluorescent proteins, more markers and promoter substitution cassettes. Yeast *21*: 947-962, 2004.
37 Caydasi AK and Pereira G: Spindle alignment regulates the dynamic association of checkpoint proteins with yeast spindle pole bodies. Dev Cell *16*: 146-156, 2009.
38 Staunton JE, Slonim DK, Coller HA, Tamayo P, Angelo MJ, Park J, Scherf U, Lee JK, Reinhold WO, Weinstein JN, Mesirov JP, Lander ES and Golub TR: Chemosensitivity prediction by transcriptional profiling. Proc Natl Acad Sci USA *98*: 10787-10792, 2001.
39 Hou J, Wang D, Zhang R and Wang H: Experimental therapy of hepatoma with artemisinin and its derivatives: *in vitro* and *in vivo* activity, chemosensitization, and mechanisms of action. Clin Cancer Res *14*: 5519-5530, 2008.
40 Sundar SN, Marconett CN, Doan VB, Willoughby JA Sr. and Firestone GL: Artemisinin selectively decreases functional levels of estrogen receptor-alpha and ablates estrogen-induced proliferation in human breast cancer cells. Carcinogenesis *29*: 2252-2258, 2008.
41 Willoughby JA Sr, Sundar SN, Cheung M, Tin AS, Modiano J and Firestone GL: Artemisinin blocks prostate cancer growth and cell cycle progression by disrupting Sp1 interactions with the cyclin-dependent kinase-4 (CDK4) promoter and inhibiting CDK4 gene expression. J Biol Chem *284*: 2203-2213, 2009.
42 Kramer A, Neben K and Ho AD: Centrosome aberrations in hematological malignancies. Cell Biol Int *29*: 375-383, 2005.

43 Fukasawa K: Centrosome amplification, chromosome instability and cancer development. Cancer Lett *230*: 6-19, 2005.
44 Uetake Y and Sluder G: Cell cycle progression after cleavage failure: mammalian somatic cells do not possess a 'tetraploidy checkpoint'. J Cell Biol *165*: 609-615, 2004.
45 Knutsen T, Gobu V, Knaus R, Padilla-Nash H, Augustus M, Strausberg RL, Kirsch IR, Sirotkin K and Ried T: The interactive online SKY/M-FISH & CGH database and the Entrez cancer chromosomes search database: linkage of chromosomal aberrations with the genome sequence. Genes Chromosomes Cancer *44*: 52-64, 2005.
46 Lens SM, Wolthuis RM, Klompmaker R, Kauw J, Agami R, Brummelkamp T, Kops G and Medema RH: Survivin is required for a sustained spindle checkpoint arrest in response to lack of tension. EMBO J *22*: 2934-2947, 2003.
47 Ruchaud S, Carmena M and Earnshaw WC: Chromosomal passengers: conducting cell division. Nat Rev Mol Cell Biol *8*: 798-812, 2007.
48 Vader G, Kauw JJ, Medema RH and Lens SM: Survivin mediates targeting of the chromosomal passenger complex to the centromere and midbody. EMBO Rep *7*: 85-92, 2006.
49 Sandall S, Severin F, McLeod IX, Yates JR 3rd, Oegema K, Hyman A and Desai A: A Bir1-Sli15 complex connects centromeres to microtubules and is required to sense kinetochore tension. Cell *127*: 1179-1191, 2006.
50 Carvalho A, Carmena M, Sambade C, Earnshaw WC and Wheatley SP: Survivin is required for stable checkpoint activation in taxol-treated HeLa cells. J Cell Sci *116(Pt 14)*: 2987-2998, 2003.
51 Honda R, Korner R and Nigg EA: Exploring the functional interactions between Aurora B, INCENP, and survivin in mitosis. Mol Biol Cell *14*: 3325-3341, 2003.
52 Morrow CJ, Tighe A, Johnson VL, Scott MI, Ditchfield C and Taylor SS: Bub1 and aurora B cooperate to maintain BubR1-mediated inhibition of APC/CCdc20. J Cell Sci *118*: 3639-3652, 2005.
53 D'Avino PP, Savoian MS and Glover DM: Cleavage furrow formation and ingression during animal cytokinesis: a microtubule legacy. J Cell Sci *118*: 1549-1558, 2005.
54 Barr FA, Sillje HH and Nigg EA: Polo-like kinases and the orchestration of cell division. Nat Rev Mol Cell Biol *5*: 429-440, 2004.
55 Lane HA and Nigg EA: Antibody microinjection reveals an essential role for human polo-like kinase 1 (Plk1) in the functional maturation of mitotic centrosomes. J Cell Biol *135*: 1701-1713, 1996.
56 Mager WH and Winderickx J: Yeast as a model for medical and medicinal research. Trends Pharmacol Sci 26: 265-273, 2005.
57 Musacchio A and Hardwick KG: The spindle checkpoint: structural insights into dynamic signalling. Nat Rev Mol Cell Biol *3*: 731-741, 2001.
58 Larsen NA, Al-Bassam J, Wei RR and Harrison SC: Structural analysis of Bub3 interactions in the mitotic spindle checkpoint. Proc Natl Acad Sci USA *104*: 1201-1206, 2007.

Received September 4, 2010
Revised October 2, 2010
Accepted October 4, 2010